



Modulation of fibrillation of hIAPP core fragments by chemical modification of the peptide backbone

Maria Andreasen^a, Søren B. Nielsen^a, Tina Mittag^b, Morten Bjerring^b, Jakob T. Nielsen^b, Shuai Zhang^c, Erik H. Nielsen^b, Martin Jeppesen^a, Gunna Christiansen^d, Flemming Besenbacher^c, Mingdong Dong^c, Niels Chr. Nielsen^b, Troels Skrydstrup^{b,*}, Daniel E. Otzen^{a,**}

^a Center for Insoluble Protein Structures (inSPIN) and Interdisciplinary Nanoscience Center (iNANO), Department of Molecular Biology and Genetics, Aarhus University, Gustav Wieds Vej 10C, DK-8000 Aarhus, Denmark

^b Center for Insoluble Protein Structures (inSPIN), Interdisciplinary Nanoscience Center (iNANO), Department of Chemistry, Aarhus University, Langelandsgade 140, DK-8000 Aarhus, Denmark

^c Interdisciplinary Nanoscience Center (iNANO), Aarhus University, Ny Munkegade 118, DK-8000 Aarhus, Denmark

^d Department of Biomedicine, Aarhus University, Wilhelm Meyers Allé 4, DK-8000 Aarhus, Denmark

ARTICLE INFO

Article history:

Received 10 August 2011

Received in revised form 14 October 2011

Accepted 24 October 2011

Available online 29 October 2011

Keywords:

Amylin

Peptide analog

Amyloid formation

Seeding

Critical aggregation concentration

ABSTRACT

The well-ordered cross β -strand structure found in amyloid aggregates is stabilized by many different side chain interactions, including hydrophobic interactions, electrostatic charge and the intrinsic propensity to form β -sheet structures. In addition to the side chains, backbone interactions are important because of the regular hydrogen-bonding pattern. β -Sheet breaking peptide analogs, such as those formed by N-methylation, interfere with the repetitive hydrogen bonding pattern of peptide strands. Here we test backbone contributions to fibril stability using analogs of the 6–10 residue fibril core of human islet amyloid polypeptide, a 37 amino acid peptide involved in the pathogenesis of type II diabetes. The Phe–Gly peptide bond has been replaced by a hydroxyethylene or a ketomethylene group and the nitrogen-atom has been methylated. In addition, we have prepared peptoids where the side chain is transferred to the nitrogen atom. The backbone turns out to be extremely sensitive to substitution, since only the minimally perturbed ketomethylene analog (where only one of the $-\text{NH}-$ groups has been replaced by $-\text{CH}_2-$) can elongate wildtype fibrils but cannot fibrillate on its own. The resulting fibrils displayed differences in both secondary structure and overall morphology. No analog could inhibit the fibrillation of the parent peptide, suggesting an inability to bind to existing fibril surfaces. In contrast, side chain mutations that left the backbone intact but increased backbone flexibility or removed stabilizing side-chain interactions had very small effect on fibrillation kinetics. We conclude that fibrillation is very sensitive to even small modifications of the peptide backbone.

© 2011 Elsevier B.V. All rights reserved.

1. Introduction

Amyloid aggregates mainly composed of fibrillated protein are associated with a wide variety of diseases such as Alzheimer's and Parkinson's disease and type II diabetes [1–3]. The term amyloid is defined as an *in vivo* deposited material which displays affinity for the dye Congo Red, characteristic fibrillar electron microscopy appearance and a specific X-ray diffraction pattern [4]. In addition, a wide range of unrelated proteins with no involvement in amyloid diseases is capable of forming fibrillar aggregates with very similar and well ordered fibrillar structure [5]. This has inspired the hypothesis that the ability to form amyloid aggregates is a generic property of proteins.

Factors influencing protein fibrillation include protein hydrophobicity, electrostatic charge and the propensity to form secondary structures such as α -helix and β -sheet [6,7]. These have successfully been combined with extrinsic properties such as pH and ionic strength allowing prediction of the aggregative propensities of different amino acid sequences [7–9]. Amyloid fibril structures consist of hydrogen-bonded β -strands forming ladders, which associate laterally to make contacts between the sidechains forming a steric zipper [10,11]. Once formed, the fibrillar structures are stabilized by the very regular hydrogen-bonding patterns along the β -ladders, as can be seen from the high level of structural persistence in fibrils, corresponding to only one “misplaced” strand per 30,000 strands [12]. For this reason, interference with this backbone pattern could be expected to severely compromise fibril integrity. Indeed, one strategy to inhibit fibril growth has been to use β -breaker peptides which bind to the growing fibril interface but lack the hydrogen bonding partners that allow further extension and thus act as “terminator peptides” [13–16]. β -Breaking ability has been achieved by using α -aminobutyric acid which strongly

Abbreviations: GAVL, decapeptide SNNFGAVLSS; GGIL, decapeptide SNNFGGILSS; NFG6, hexapeptide NFGAIL; SN10, decapeptide SNNFGAILSS; ThT, thioflavin T

* Corresponding author. Tel.: +45 89 42 39 32; fax: +45 86 19 61 99.

** Corresponding author. Tel.: +45 89 42 50 46; fax: +45 86 12 31 78.

E-mail addresses: ts@chem.au.dk (T. Skrydstrup), dao@inano.au.dk (D.E. Otzen).

favors α -helical conformations and which sterically prevents β -sheet contacts, or by using peptides with modified termini. Another approach has been to modify the peptide backbone with N-methylations or introduction of bulky groups to sterically hinder the formation of hydrogen bonds [17–23]. The presence of methyl groups on the backbone amide prevents the formation of hydrogen bonds with the following peptide, and hence blocks the formation of amyloid fibrils.

Here, we report the effect of a single-site backbone modification of two peptides of length 6 and 10 residues with the sequences NFGAIL (hIAPP 22–27, denoted NF6 in this work) and SNNFGAILSS (hIAPP 20–29, denoted SN10). These peptides comprise the fibrillating core of human Islet Amyloid Polypeptide (hIAPP) [24,25]. hIAPP is a 37 amino acid peptide hormone which constitutes the major part of the pancreatic amyloid found in patients with type II diabetes [3,26,27]. Fibrils of both the hexa- and decapeptide of the fibrillating core of hIAPP have been shown to be cytotoxic toward pancreatic cell lines and this cytotoxicity and the amyloidogenicity can be blocked by double N-methylated versions of the peptides [18,19,24]. The fibril structure of the decapeptide has been solved using solid-state NMR, revealing an anti-parallel hetero zipper with an observed twist along the axis of the fibril [28,29]. As summarized in Fig. 1, we have modified the FG amide bond of the hexapeptide by the removal of the nitrogen atom from the backbone amide and introduction of a hydroxyethylene group (analog He) as well as by preparing an N-methylated version (analog Nm). Furthermore, we have synthesized and examined the retropeptid version of the decapeptide (analog Rp). Peptoids are oligomers of N-substituted glycines which are isomers of peptides but resistant toward hydrolysis by proteases [30,31] and have been found to inhibit the formation of fibrils [32]. A ketomethylene isostere of the decapeptide at the same amide bond has also been prepared and tested (analog Km). As controls, we investigated two mutants of the decapeptide, namely SNNFGAVLSS (GAVL peptide) and SNNFGGILSS (GGIL peptide), which have similar types of structural changes as the chemical analogs but at the level of side chain interactions. Hydrophobic interactions were tested by removal of a methyl group in the I \rightarrow V mutation, and the rotational freedom of the peptide backbone was examined by the A \rightarrow G mutation in the same position where the backbone is modified in the peptide analogs.

We find that even modest changes to the backbone integrity can have severe effects on the behavior of these peptides with respect to fibril formation and potential fibril morphology on a local (degree of ordering, chain packing) and more global scale (twisting, thickness). Only analog Km with the smallest change in the backbone ($-\text{NH}-$ replaced by $-\text{CH}_2-$) was able to elongate fibril seeds, and gave rise to fibrils with different secondary structure and morphology compared to the original peptide. No other peptide analog could elongate existing fibril seeds. These highlight a central role for the backbone in stabilizing the cross- β structure. Moreover, addition of any analog to wildtype fibrils was unable to prevent or limit growth of the fibrils.

2. Materials and methods

2.1. Materials

Chemicals were purchased from Sigma-Aldrich, St. Louis, Missouri and Iris Biotech GmbH, Marktredwitz, Germany. Analogs He and Km were prepared as described by us [33].

2.2. Peptide synthesis

2.2.1. General method for fully automated microwave-assisted solid phase peptide synthesis

The peptide synthesis was performed on a CEM Liberty microwave assisted peptide synthesizer using Rink amide MBHA resin (0.45 mmol/g) on a 0.1 mmol scale. The resin was swelled for 15 min in 10 mL DMF using the standard protocol of the peptide synthesizer. The coupling cycles used were the standard single coupling cycles described below:

Fmoc deprotection: 20% piperidine in DMF (7.0 mL) was added, and microwave heating was employed for 30 s. After draining, 20% piperidine in DMF (7 mL) was added again and the mixture was heated under microwave radiation for 3 min. Nitrogen gas agitation was used during heating.

Wash: Washings were performed using 7.0 mL of DMF with nitrogen gas agitation and were repeated four times.

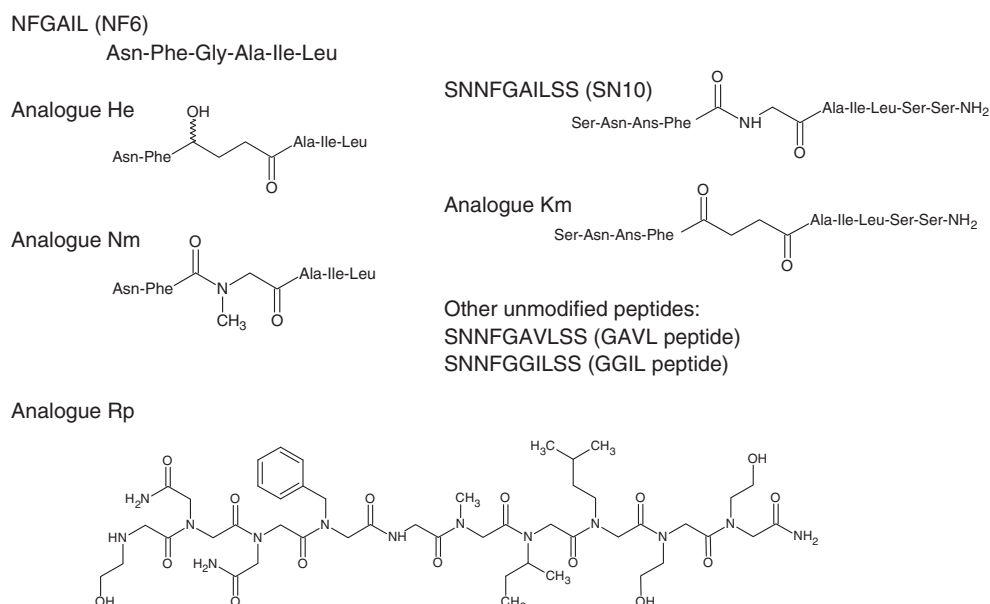


Fig. 1. Structure of SN10 and peptide analogs used in the present study. Analog He: NF6 hydroxyethylene isostere, Analog Nm: N-methylated NF6, Analog Rp: SN10 retropeptid, Analog Km: SN10 ketomethylene isostere, WT: wild-type SN10.

Peptide coupling: Amino acids were added as a 0.20 M solution in DMF (2.5 mL, 0.5 mmol), HBTU was added as a 0.50 M solution in DMF (1.0 mL, 0.5 mmol) and DIPEA was added as a 2.00 M solution in *N*-methylpyrrolidone (0.5 mL, 1.0 mmol). Microwave heating was employed for 5 min giving an end temperature of 80 °C. Nitrogen gas agitation was used during heating.

After completing the final Fmoc-deprotection cycle, the peptidyl resin was dried down by washing with CH₂Cl₂ (3 × 4 mL), then with MeOH (3 × 4 mL) and finally dried under reduced pressure. Cleavage and deprotection of the peptide was performed by treating the resin with 5 mL of TFA:H₂O:TIPS 95:2.5:2.5 (v/v) for 2 h at rt. The cleavage mixture was concentrated to approximately 1 mL under reduced pressure, followed by precipitation in cold *tert*-butyl methyl ether. Repeated centrifugation, decantation, and trituration with *tert*-butyl methyl ether (4 times) followed by lyophilization gave the crude peptide.

2.2.2. RP-HPLC

Analytical RP-HPLC was performed using an Agilent 1100 system with a Phenomenex Kinetex column (C18, 4.6 mm ID × 150 mm, 2.6 μm, 100 Å) operated at a flow rate of 1 mL/min at 25 °C. Semi-preparative RP-HPLC purification was performed on an Agilent 1200 system with a Agilent Zorbax SB column (C18, 9.8 mm ID × 250 mm, 5 μm, 300 Å) operated at a flow rate of 5 mL/min at 25 °C. The solvent system: A = 0.1% TFA in H₂O, B = 0.1% TFA in acetonitrile.

2.2.3. NF6 peptide (H-NFGAIL-OH)

The peptide was synthesized according to the general method except that the synthesis was performed at a 0.25 mmol scale using a pre-loaded Fmoc-Leu-Wang resin (0.75 mmol/g). The Crude peptide (116 mg) was dissolved in 10% AcOH and purified employing a linear gradient of 5–60% solvent B in solvent A, yielding the title compound in a purity of 94.5%. $t_R = 16.73$ min (Agilent C18 Stablebond, over 50 min). MALDI-TOF MS: C₃₀H₄₇N₇O₈ [M + Na⁺]; calculated 656.34, found 656.39.

2.2.4. SN10 peptide (H-SNNFGAILSS-NH₂)

The peptide was synthesized according to the general method. The Crude peptide (75 mg) was dissolved in 10% AcOH and purified employing a linear gradient of 5–40% solvent B in solvent A, yielding 23.3 mg (22%) of the title compound in a purity of 90.2%. $t_R = 9.71$ min (Phenomenex Kinetic, over 15 min). MALDI-TOF MS: C₄₃H₆₉N₁₃O₁₅ [M + Na⁺]; calculated 1030.49, found 1030.50.

2.2.5. GAVL peptide (H-SNNFGAVLSS-NH₂)

The peptide was synthesized according to the general method. The Crude peptide (94 mg) was dissolved in 10% AcOH and purified employing a linear gradient of 5–50% solvent B in solvent A, yielding 34.5 mg (35%) of the peptide in a purity of 91.7%. $t_R = 7.64$ min (Phenomenex Kinetic, over 15 min). MALDI-TOF MS: C₄₂H₆₇N₁₃O₁₅ [M + K⁺]; calculated 1032.45, found 1032.55.

2.2.5.1. GGIL peptide (H-SNNFGGILSS-NH₂). The peptide was synthesized according to the general method. The Crude peptide (90 mg) was dissolved in 10% AcOH and purified employing a linear gradient of 5–50% solvent B in solvent A, yielding 33.8 mg (33%) of the title compound in a purity of 88.1%. $t_R = 8.26$ min (Phenomenex Kinetic, over 15 min). MALDI-TOF MS: C₄₂H₆₇N₁₃O₁₅ [M + Na⁺]; calculated 1016.48, found 1016.70.

2.2.6. Analog Nm (N-methylated derivative L-Asparaginyl-L-phenylalanyl-L-phenyl-L-glycyl)-L-alanyl-L-isoleucyl-L-leucinamide)

H-NF(N-Me)GAIL-OH, was synthesized according to the general method except pre-loaded Fmoc-Leu-Wang resin was employed

(0.75 mmol/g). The following protected unmodified and modified natural amino acids were used: Fmoc-Leu-OH, Fmoc-Ile-OH, Fmoc-Ala-OH, Fmoc-(*N*-Me)Gly-OH, Fmoc-Phe-OH, and Fmoc-Asn(Trt)-OH. The cleavage and deprotection of the peptide was performed by treating the resin with 2 mL of TFA:H₂O:TIPS 95:2.5:2.5 (v/v) for a total of 5 h (2 × 2.5 h). The crude peptide was dissolved in H₂O and purified by semi-preparative using a linear gradient of 0–60% solvent B in solvent A. This provided the title compound (31 mg, 48%, 98% purity). HRMS C₃₁H₄₉N₇O₈ [M + H⁺]; calculated: 648.3721, found: 648.3724.

2.2.7. Analog Rp (H-NSer-NSer-NLeu-NIle-NAla-Gly-NPhe-NAsn-NAsn-NSer-NH₂)

This peptid was synthesized by manual solid-phase organic synthesis using a Rink amide MBHA resin (0.2 mmol) [32]. The synthesis was performed using a combination of the monomer and submonomer approach. Residues mimicking serine, asparagine, phenylalanine, isoleucine, and leucine were performed using the submonomer approach, while Fmoc-sarcosine-OH was applied for the synthesis of the alanine residue by the monomer approach. Submonomer method: The acylations were performed by addition of bromoacetic acid (4 mL, 0.5 M in DMF, 2.0 mmol) and DIC (2.2 mL, 1.0 M in DMF, 2.2 mmol) to the resin followed by vigorous shaking 20 °C for 30 min, then the reaction mixture was filtered and the reaction was repeated. Nucleophilic substitution of bromide was performed by reaction of a primary amine (4 mL, 1 M in DMSO, 4 mmol) for 1 h at 20 °C. The following amines were used: benzylamine for NPhe, glycinamide hydrochloride for NAsn, isobutylamine for NLeu, racemic *sec*-butylamine for NIle and TBDMS-protected ethanolamine for NSer. *N*-methyl morpholine (2.0 mmol) was added in reactions with glycinamide hydrochloride. Monomer method: Fmoc-sarcosine-OH (187 mg, 0.60 mmol) and Fmoc-glycine-OH (178 mg, 0.6 mmol) were attached to the growing peptid chain using standard solid phase peptide coupling conditions: HBTU (220 mg, 0.58 mmol), HOBt (81 mg, 0.6 mmol) and DIPEA (209 μL, 1.2 mmol) in DMF (4 mL) over 1 h [34]. This was followed by removal of the Fmoc protection groups by repeated treatment of the resin with 20% piperidine in DMF (5 min × 3). After attachment of the last residue, the resin was dried down by washing with CH₂Cl₂ (3 × 4 mL), then with MeOH (3 × 4 mL) and finally dried under reduced pressure. Cleavage and deprotection of the peptide was performed by treating the resin with 5 mL of TFA:H₂O:TIPS 95:2.5:2.5 (v/v) for 2 h. The cleavage mixture was concentrated to approximately 1 mL under reduced pressure, followed by precipitation in cold *tert*-butyl methyl ether. Repeated centrifugation, decantation, and trituration (4 times) followed by lyophilization gave the crude peptide. The crude mixture was dissolved in H₂O and purified by semi-preparative HPLC using a linear gradient of 10–60% solvent B in solvent A. This provided the title compound (46 mg, 22%). HRMS C₄₇H₇₇N₁₃O₁₅ [M + H⁺]; calculated: 1050.5584, found: 1050.5585.

2.3. Preparation of samples

All decapeptides (SN10, mutants and analogs) were dissolved in DMSO to a concentration of 25 mM. Hexapeptides (NF6 and analogs) were dissolved in DMSO to a concentration of 1000 mM. All peptides were subsequently diluted 1:100 into 50 mM HEPES buffer pH 7.2 and filtered through a 0.2 μm filter unit. Seeds of preformed fibrils were produced by centrifugation of fibrils for 30 min at 13,000 rpm in a tabletop centrifuge. The supernatant was removed and the fibrils were re-suspended in 50 mM HEPES buffer pH 7.2 to a concentration of 10 mM for NF6 fibrils and 0.25 mM for SN10 fibrils. Seeds of preformed fibrils were produced by sonication for 10 s at 30% amplitude with a Bendelin Sonopuls HD 2070 sonication probe (Buch & Holm). For all seeded fibrillation experiments, 5% preformed fibril seeds were used to seed the next generation of fibrils.

2.4. Fibrillation of peptides and analogs

Thioflavin T (ThT) was added to the protein solution to a final concentration of 40 μM and the protein solution was transferred to a 96-well black Costar polystyrene microtiter plate, sealed to prevent evaporation and placed in an Infinite M200 plate reader (Tecan Nordic AB). When fibril seeds were present, these were added immediately before the plate was sealed. The plate was incubated at 37 °C and the ThT fluorescence (excitation 450 nm, emission 482 nm) was measured every 5 min with 3 min shaking between each reading.

2.5. Protein concentration analysis

The concentration of peptides in the supernatant after fibrillation and centrifugation for 30 min at 13,000 rpm in a tabletop centrifuge was analyzed using the BCA Protein Assay Reagent kit (Thermo Fisher Scientific) according to the manufacturers' recommendations. A standard curve was made from a stock solution of the parent peptides with known concentration. The concentration of NF6 was also examined by absorbance at 220 nm on a Nanodrop spectrophotometer ND1000 (Saveen Werner), also using a standard curve made from a stock solution with known concentration.

2.6. Atomic force microscopy (AFM)

Aliquots of 5 μL fibril solution were deposited onto freshly cleaved mica surface, air dried for 5 min and finally dried with N_2 . All images were captured using a Nanoscope V MultiMode SPM (Veeco Instruments) under ambient conditions. Ultrasharp silicon cantilevers with a typical resonance frequency of 300 kHz, a spring constant of 26 N/m and a normal tip radius of 7 nm (triangular, OMCL-AC160TS-E3, Olympus) were used. AFM imaging was performed in tapping mode at scan frequency of 1 Hz with minimal loading forces of 100 pN applied and optimized feedback parameters. The resolution of all AFM images shown is 512×512 pixels per image. The images were flattened and analyzed automatically using the Scanning Probe Image Processor software (SPIPTM, Image Metrology ApS, version 5.1.3).

2.7. Transmission Electron Microscopy (TEM)

Aliquots of 5 μL of fibril solution were mounted on 400-mesh carbon coated, glow discharged nickel grids for 30 s. The grids were washed with one drop of double distilled water and stained with three drops of 1% phosphotungstic acid pH 7.2. Samples were inspected in a JEOL 1010 transmission electron microscope at 60 keV. Images were obtained using an electron sensitive Olympus KeenView CCD camera.

2.8. Far-UV circular dichroism (CD) spectroscopy

All samples were spun down in a tabletop centrifuge at 13,000 rpm for 30 min. Samples with visible pellet were resuspended in 10 mM HEPES buffer pH 7.2. All samples were subjected to sonication for 2 s at 60% amplitude with a Bendelin probe and inspected for the presence of visible aggregates in the cuvette prior to analysis. CD wavelength spectra from 250 nm to 200 nm with a step size 0.2 nm, bandwidth of 2 nm and scan speed of 50 nm/min were recorded at 25 °C with a J-810 CD-spectrometer (Jasco) using a 1 mm quartz cuvette (Hellma). Five spectra were averaged for each sample and the buffer spectra were subtracted.

2.9. Fourier transform infra-red (FTIR) spectroscopy

FTIR spectroscopy was performed using a Tensor27 FTIR spectrometer (Bruker) equipped with Attenuated Total Reflection

accessory with a continuous flow of N_2 gas. All samples were dried with N_2 gas. 64 interferograms were accumulated at a spectral resolution of 2 cm^{-1} . Following self deconvolution, the intensity was modeled by Gaussian curve fitting using the OPUS 5.5 software. Peak positions were assigned where the second order derivative had local minima.

2.10. X-ray fiber diffraction and analysis

Fiber diffraction specimens were prepared on a stretch frame using 5 μL fibril suspensions of approximately 2.5 mg/mL. Diffraction data fibers were collected at room temperature using a fixed wavelength of 0.8015 Å on a 165 mm MAR-Research CCD detector (Hamburg, Germany) on the beamline X13 (EMBL-outstation at DESY, Hamburg, Germany) using exposure times from 5 to 45 s. The sample to detector distance was set at 300 mm. The collected diffraction patterns were centered, background corrected by local box averaging and 60° radial scans of meridional and equatorial reflections were obtained using Clearer v2.0 for Java v1.5 [35].

2.11. Solid-state NMR spectroscopy

The samples for solid-state NMR spectroscopy were prepared by centrifugation of fibril suspensions, removing the supernatant, and transferring the fibrils to 4 mm (outer diameter) rotors. The samples contained approximately 4 mg (SN10), 9 mg (GAVL) and 11 mg (GGIL) of fibrillated peptide. Natural abundance ^{13}C solid state NMR spectra were acquired using ^1H - ^{13}C cross polarization in combination with 12 kHz magic angle spinning (CP/MAS) applying 23,000 scans per spectrum and repetition delays of 3 s.

3. Results

3.1. Fibrillation of IAPP-derived peptides is very sensitive to backbone modification

We follow the kinetics of fibril formation by monitoring the increase in fluorescence of the fibril-binding dye ThT. Fibrillation of the parent peptides NFGAIL (NF6) and SNNFGAILSS (SN10) followed a nucleation dependent pathway. This can be seen in two ways. Firstly, there is a characteristic lag phase in the accumulation of the ThT signal (Fig. 2A), which is generally attributed to the build-up of a critical amount of elongation-competent nuclei [36]. Secondly, the duration of this lag phase (the lag-time) was reduced by the addition of preformed fibril seeds. In the absence of fibril seeds, the lag-time of NF6 was found to range from 6 to 10 h while the lag-time of SN10 was 5.3 ± 0.3 h. The presence of 5% fibril seeds was found to completely eliminate the lag-time for both peptides (Fig. 2B). As expected, the presence of preformed fibril seeds does not change the secondary structure of the fibrils formed (Fig. 2C).

Analog Km is the only decapeptide analog capable of elongating existing fibril seeds from the parent peptide (Fig. 2B). Over a 70 h period, none of the other peptide analogs display an increase in ThT fluorescence upon incubation with preformed fibril seeds of the parent peptide. Far-UV CD spectra of these fibrils show very low ellipticity similar to monomeric peptide, precluding further analysis (Fig. 3A and B). Although capable of elongating fibril seeds, analog Km is not capable of forming fibrils in the absence of seeds of the parent peptide or in the presence of fibril seeds of Km (Fig. 2B). This indicates that analog Km needs the scaffold of existing well ordered fibrils in order to form the proper hydrogen bonding pattern needed for fibril formation. Interestingly, the secondary structure of the fibrils formed by analog Km is different from that of fibrils of SN10 as seen from the FTIR spectra (Fig. 3C). They contain less β -sheet structure (both amyloid and intermolecular) and also less β -turn structure, while the content of α -helix like structure is considerably higher (Table 1).

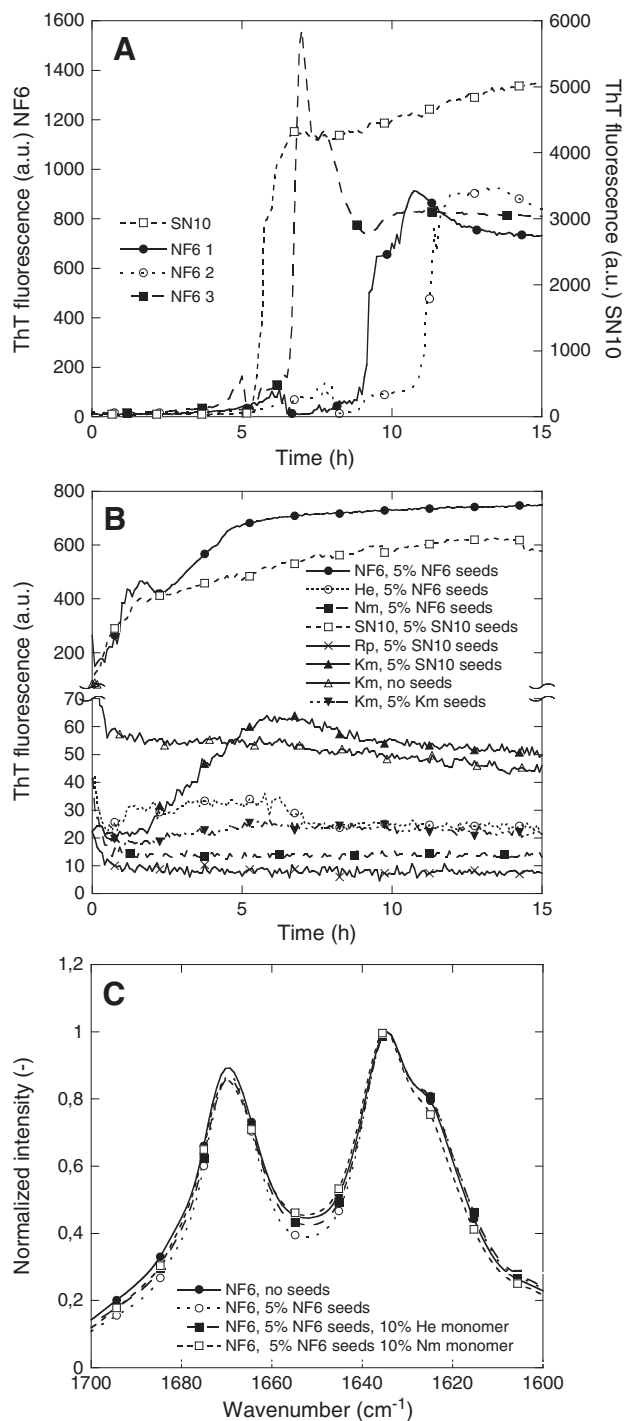


Fig. 2. Fibrillation of NF6, SN10 and analogs. A: Non-seeded fibrillation of SN10 and NF6. The ThT fluorescence of single fibrillations of NF6 is plotted against the left y-axis while the ThT fluorescence of a triplicate of SN10 is plotted against the right y-axis. The gain setting for the experiment with SN10 is higher than that of the rest of the experiments reported in the present study giving rise to higher signals. B: Seeded fibrillation of SN10, NF6 and analogs, and non-seeded fibrillation of analog Km. In the seeded fibrillation wt seeds were used of the same residue length as the monomer (*i.e.* SN10 or NF6). C: Normalized FTIR signal of fibrils of NF6. The only analog capable of elongating fibril seeds of parent fibrils is analog Km.

3.2. Side chain mutations have much smaller effects on fibrillation

In contrast to the backbone-modified peptides, both decapeptide mutants GGIL and GAVL fibrillate in the presence as well as in the

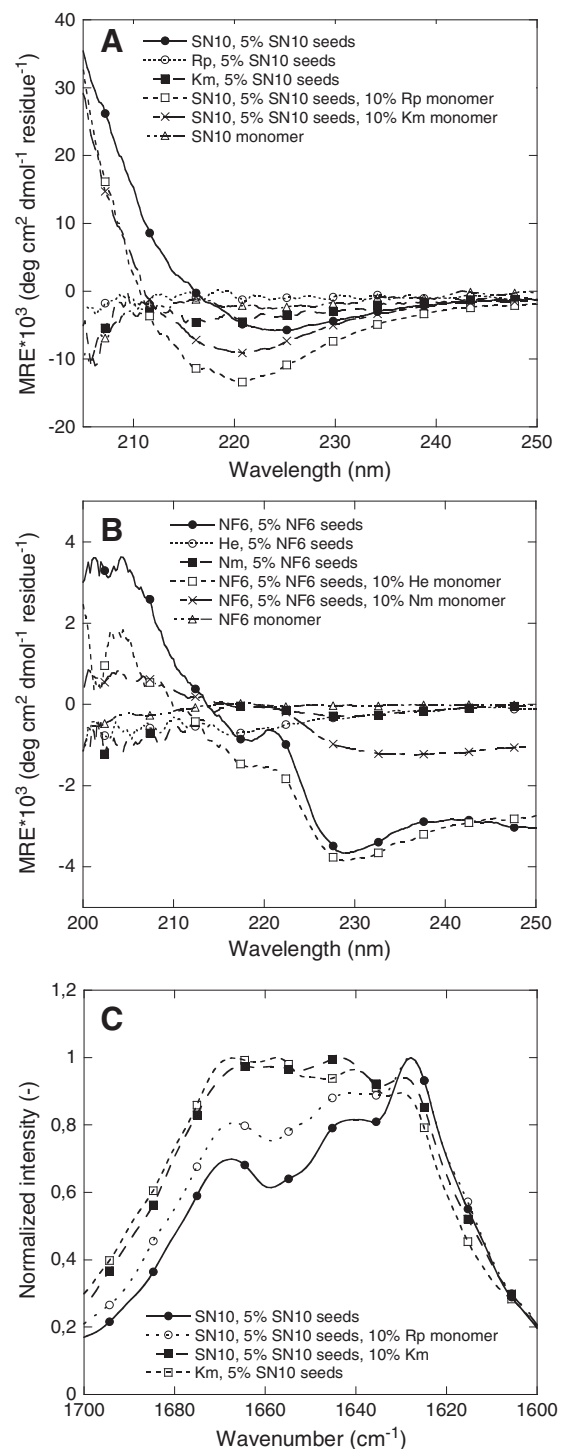


Fig. 3. Analysis of the secondary structure of fibrils by far-UV CD and FTIR. A: Far-UV CD of fibrils of SN10 analogs. B: Far-UV CD of fibrils of NF6 and NF6 analogs. C: Normalized FTIR signal of fibrils of SN10 and SN10 analogs.

absence of SN10 fibril seeds (Fig. 4A). The fibrillation time course of the GGIL peptide is essentially identical in the absence and presence of SN10 fibrils, while there is a clear decrease in lag time for GAVL. This indicates that GAVL, but not GGIL, elongates the SN10 fibril seeds. For both peptide mutants, far-UV CD spectra indicate that the presence of SN10 seeds does not alter the secondary structure of the ensuing fibrils. However, both FTIR and far-UV CD spectra show that the secondary structure of fibrils of both mutants are different from

Table 1
Contents of secondary structural elements of fibrils obtained from deconvolution of FTIR spectra of fibrils according to references [50,51].

Sample	Amyloid β -sheet	β -Sheet	β -Turn	α -Helix	Random coil
SN10, 5% SN10 seeds	33.6	31.4	30.5	0.6	–
SN10, 5% SN10 seeds, 10% Rp monomer	20.7	46	32.9	0.2	–
SN10, 5% SN10 seeds 10% Km monomer	21.3	33.3	34.2	10.9	–
D, 5% SN10 seeds	18.2	28	6.4	29.2	–
SN10, 5% SN10 seeds	34.5	25	36.2	2.5	–
GGIL, 5% SN10 seeds	32.4	29.1	35.9	1.8	–
GAVL, 5% SN10 seeds	36.5	26.4	35.2	0.9	–
SN10, 5% SN10 seeds, 10% GGIL monomer	32.8	5.4	6	29.2	6.6
SN10, 5% SN10 seeds, 10% GAVL monomer	26.4	20.7	34.3	4.3	11.6
NF6	18.7	33.8	34.3	–	–
NF6, 5% SN10 seeds	21.2	33.3	35.5	–	–
NF6, 5% SN10 seeds, 10% He monomer	20	32.4	34.2	–	–
NF6 5% SN10 seeds, 10% Nm monomer	18	32.1	32.5	–	–

that of SN10 fibrils (Fig. 4B and C), particularly for GGIL. A small change in the secondary structure of SN10 fibrils, involving a ~ 1.5 nm blue shift of the minimum around 222.5 nm, is also seen in

the far-UV CD spectra when GGIL is present during the fibrillation (Fig. 4C). This indicates that the mutant can leave an imprint on the SN10 fibrils formed. Taken together, this indicates even the small changes in hydrophobic interaction and the rotational freedom around the peptide backbone can have a significant impact on the structure of the fibrils formed.

Peptides lacking hydrogen bonding potential might act as β -breakers and thus inhibit fibrillation by blocking elongation. However, this was not observed for any of the hexa- or decapeptide analogs synthesized for this study. The addition of 10% of peptide analogs or 10% peptide mutant to the parent peptide during fibrillation did not affect the ThT fluorescence time curve (Fig. 4D). This might be taken to indicate that the parent peptide fibrillates without any interaction with the peptide analog or peptide mutant. However, as seen for the GGIL and GAVL peptides above, the structure of the fibrils formed indicates that in some instances the peptide analogs and the mutants change the fibril structure. In the case of NF6, the presence of peptide analogs does not affect the secondary structure as evident from the FTIR data (Fig. 2C). This can also be seen for SN10 fibrillated in the presence of analog Rp. But in the case of SN10 both with analog Km and mutants, the secondary structure of the fibrils is affected by the presence of analogs and mutants, respectively (Figs. 3C and 4B and Table 1). The fibrils of SN10 made with 10% of analog Km have a secondary structure which is in between SN10 fibrils and Km fibrils with respect to both the content of amyloid β -sheet and α -helix. This indicates that the analog is capable of being incorporated into fibrils of SN10 made from preformed SN10 fibril seeds.

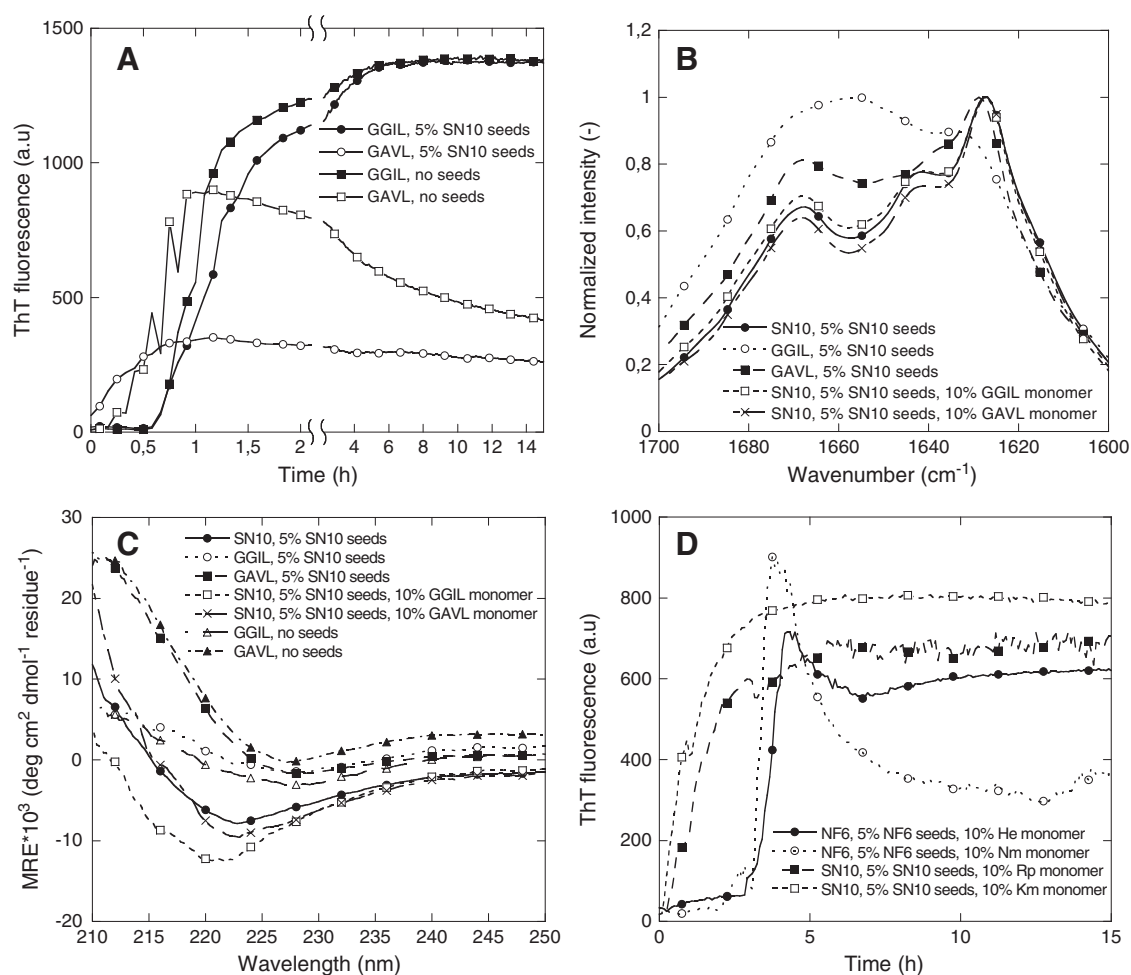


Fig. 4. Fibrillation of SN10 mutants and inhibition of fibrillation of the parent peptide in the presence of analogs. A: Fibrillation of SN10 mutants with and w/o fibril seeds. The mutants are capable of fibrillation both with and w/o fibril seeds. B: Normalized FTIR signal of fibrils of SN10 mutants. C: Far-UV CD of fibrils of SN10 mutants. D: Fibrillation of parent peptide in the presence of analogs. No inhibition of the fibrillation is observed.

3.3. The critical concentration for fibrillation is very sensitive to peptide length

The critical concentration (c_c) for fibrillation to occur can be determined by centrifugation and subsequent measurements of the concentration of peptide in the supernatant. If fibrillation is viewed as a phase transition between soluble monomer and insoluble fibrils, this concentration is the initial monomer concentration which needs to be exceeded for fibrillation to occur, and it is the concentration of monomers in the solution after fibrillation has ended [37]. The lower the c_c , the more easily the peptide is incorporated into the growing fibrils [38]. The c_c of NF6 and SN10 were determined to be 6.8 ± 0.3 and 0.041 ± 0.001 mM, respectively (Table 2). This more than 100-fold difference in c_c explains why much higher concentrations of NF6 are required for fibrillation compared to SN10. For analog Km seeded with SN10, the c_c was found to be 0.091 ± 0.018 mM, indicating that the backbone modification leads to a relatively modest ~2-fold destabilization of the fibrils, corresponding to a decrease in fibril stability by $\Delta\Delta G_{\text{fib}} = -RT \ln(0.041/0.091) = -0.48$ kcal/mol. The c_c of the two SN10 mutants does not change significantly when 5% SN10 fibril seeds are present (Table 2). This suggests that the slight alteration in secondary structure caused by the SN10 seeds does not affect the stability of the fibrils.

3.4. Structural analysis of the different fibrils highlights different morphologies

Synchrotron X-ray diffraction patterns and the spacing of the reflections were obtained from both partially aligned fibril samples originating from seeded (Fig. 5A and B) or non-seeded fibrils (data not shown). X-ray diffraction patterns often yield simple patterns with 4.7–4.8 Å meridional reflections and ~8–10 Å equatorial reflections. These arise from molecular spacings corresponding to hydrogen-bonded β -strands arranged perpendicular to the fiber axis and the β -sheet distance, respectively [39].

In this study, the alignment of fibers of SN10, the GGIL and GAVL mutant peptides and analog Km was not sufficient to obtain clearly resolved meridional and equatorial reflections (Fig. 5B). However, radial scans of the recorded patterns revealed essentially similar reflections including a 4.78 Å peak corresponding to the β -strand spacing and a diffuse reflection of weak intensity at ~8.7–8.8 Å characteristic for the amyloid cross- β structure. The position of these reflections is in good agreement with previous work by other groups [39,29]. This suggests that the changes imposed to the polypeptide chain do not alter the overall amyloid structure.

The radial scans further revealed subtle differences in the ~4.57–4.61 Å region (Fig. 5B). More specifically, fibrils from SN10 and the GGIL mutant, which showed the same ability to elongate seeds as SN10 (Fig. 4A), gave rise to a reflection at 4.61 Å. This particular distance was reduced to ~4.57 Å in GAVL which also showed a reduced Thioflavin T fluorescence in elongation assays compared to GGIL (Fig. 4A). The ~4.57–4.61 Å reflection was not detected in samples of the Km analog seeded with wt fibril seeds. This analog did not fibrillate on its own but required seeding with SN10, suggesting that a molecular interaction related to this distance may represent a

Table 2

Critical concentration of fibrillation and corresponding ΔG_{fib} values for the peptides analyzed.

Sample	C_c (mM)	ΔG_{fib} (kJ/mol)
NF6	6.8 ± 0.3	-3.1
SN10	0.041 ± 0.0005	-6.2
Analog Km, 5% SN10 seeds	0.091 ± 0.018	-5.7
GGIL peptide	0.061 ± 0.014	-6.0
GAVL peptide	0.073 ± 0.002	-5.9
GGIL, 5% SN10 seeds	0.044 ± 0.005	-6.2
GAVL, 5% SN10 seeds	0.052 ± 0.009	-6.1

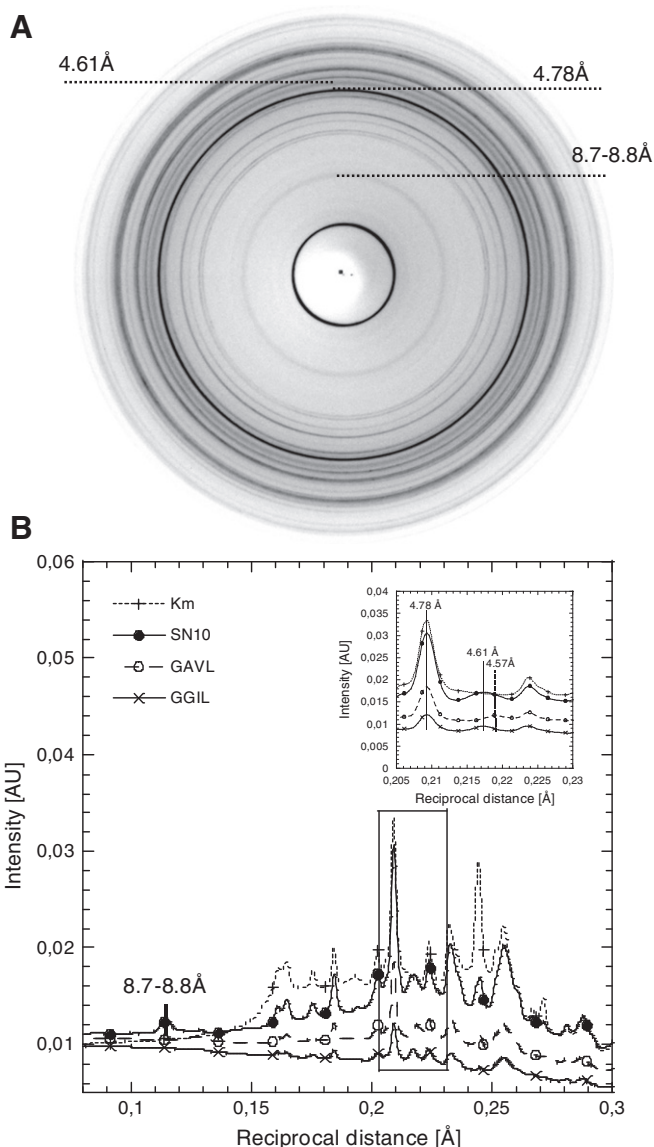


Fig. 5. Analysis of X-ray fiber diffraction pattern of fibers prepared from seeded SN10, GAVL, GGIL and analog Km samples. (A) Diffraction pattern of seeded SN10. (B) Radial scans of diffraction patterns from panel A with the reflection at ~4.78 and 8.7–8.8 Å characteristic for amyloid fibrils (highlighted in the zoomed insert) and subtle differences between samples in the 4.57–4.61 Å region.

structural motif important for promoting fibrillation in the absence of preformed seeds. It is not clear which molecular packing correspond to the 4.55–4.61 Å reflections. However, their existence and variability indicate subtle differences in the packing of the fibrils. Apart from this lacking reflection in fibrils of analog Km, the different fibrils show highly similar reflections indicative of a common overall structure, despite the changes imposed on the polypeptide chain.

3.5. ssNMR spectra confirm that different peptides form different structural classes of fibrils

To further explore variations in the fibril structures at the atomic level, we acquired one-dimensional solid-state NMR spectra for representative fibrils. We note here that ^{13}C natural abundance NMR is not a high-sensitive technique, and the spectra should by no means be compared with spectra of ^{13}C labeled peptides. More detailed investigations as determination of complete high-resolution 3D structures require ^{13}C and ^{15}N labeling of the peptides in combination with multidimensional spectra. However, the chemical shift patterns (line splittings etc.) in

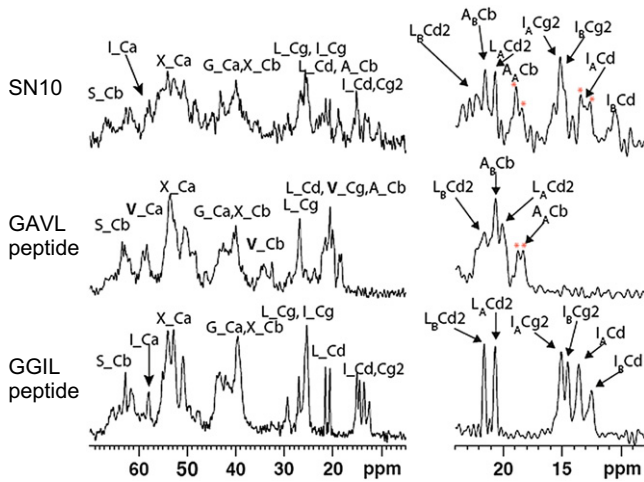


Fig. 6. 1D ^{13}C CP/MAS solid-state NMR spectra of SNNFGAILSS wild type (top) and mutants (mutated residue shown in bold). Assignments are provided along with each spectrum. Magnification of the methyl region (24–8 ppm) of the spectra is shown in the right panel. In the magnifications asymmetric pairs of the same carbon are indicated by A/B subscripts. Additional splitting of the A/B form, if present, is highlighted with red asterisks.

simple 1D ^{13}C spectra acquired using natural abundance fibril samples can provide some indications on fibril symmetries and local order as demonstrated previously by Nielsen et al. [28]. From the spectra of the SN10, GAVL, and GGIL fibrils in Fig. 6, it is seen that they all feature line splitting, suggesting that fibrils are not totally symmetric. These splitting patterns can distinguish between different fibril classes but not specifically assign fibrils to a unique symmetry class without the use of multidimensional solid state NMR data, as was done for the SN10 fibril [28]. For all samples, these splitting were most apparent for

the well resolved Ile, Leu and Ala methyl groups, revealing splitting into doublets and further doublet-doubling in some of the cases, whereas putative splitting for other resonances such as C α could not be confirmed using 1D ^{13}C NMR spectra due to spectral overlap. For SN10, the resonances were assigned previously using standard approaches based on 2D solid-state NMR spectra [28]. We observe a doubling of the resonances, and for A $_A$ C β and I $_A$ C δ a further doubling is observed (Fig. 6 top panel) consistent with the original assignment of SN10 as an anti-parallel ladder hetero zipper class [28]. A related pattern is found for the GAVL mutant (Fig. 6 middle panel), revealing doubling of LC δ 2 and AC β resonances and a further splitting of A $_A$ C β as for the wild-type. A likely interpretation is that this mutant adopts the same fibril zipper class as for the wild-type SN10 fibrils. Conversely, for GGIL (Fig. 6 bottom panel) we observe a distinct splitting into two resonances, which are well resolved for the Ile, Leu and Ala methyl groups, but in this case no further splitting of the doublets could be confirmed. The lack of further splitting could indicate a different zipper class for this mutant. This interpretation is supported by the observation of significant changes of chemical shifts for the Ile methyl groups (up to 1.8 ppm for IBC δ) which may be due to different packing in the zipper. This alternative zipper class could be a parallel ladder-hetero zipper arrangement where the side chains of a certain residue point into the zipper in one ladder, while the side chains of the same residue point out of the zipper in the opposite ladder. However, the 1D spectra do not completely exclude further minor splitting of the signals, which would be compatible with antiparallel ladder fibril symmetries. Both of these mutants particularly GGIL, give very homogenous fibrils with well resolved signals, indicative of a high local order.

In order to analyze the structural features of fibrils further, we turned to TEM and AFM imaging. The morphology of the fibrils of SN10 monomers formed in the absence and in the presence of fibril seeds both show long, un-branched, twisted ribbon-like fibrils (Figs. 7 and 8 and summarized in Table 3). A similar morphology is

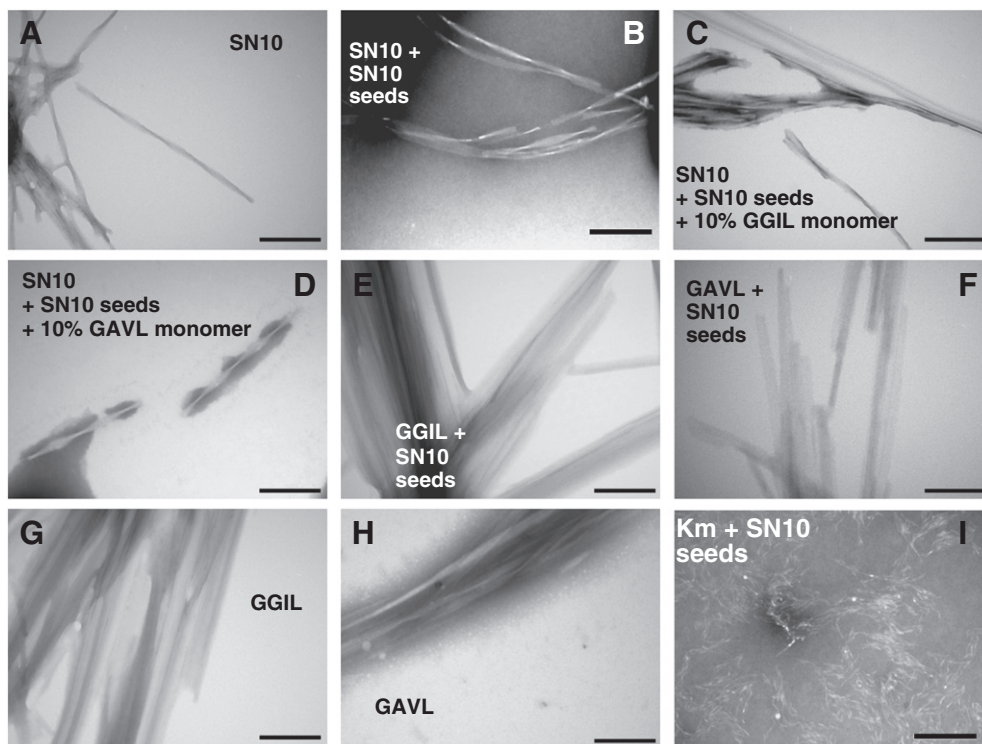


Fig. 7. Morphology of fibrils examined by Transmission Electron Microscopy. Upper panel: A: Fibrils of SN10; B: Fibrils of SN10 formed in the presence of 5% fibril seeds; C: Fibrils of SN10 formed in the presence of 5% fibril seeds and 10% GGIL. Middle panel: D: Fibrils of SN10 formed in the presence of 5% fibril seeds and 10% GAVL; E: Fibrils of GGIL formed in the presence of 5% SN10 fibril seeds; F: Fibrils of GAVL formed in the presence of 5% SN10 fibril seeds. Bottom panel: G: Fibrils of GGIL; H: Fibrils of GAVL; I: Fibrils of analog Km formed in the presence of 5% SN10 fibril seeds. The scale bar represents 200 nm. The morphology of the fibrils is greatly dependent on the peptide fibrillating both in the presence and absence of preformed fibril seeds.

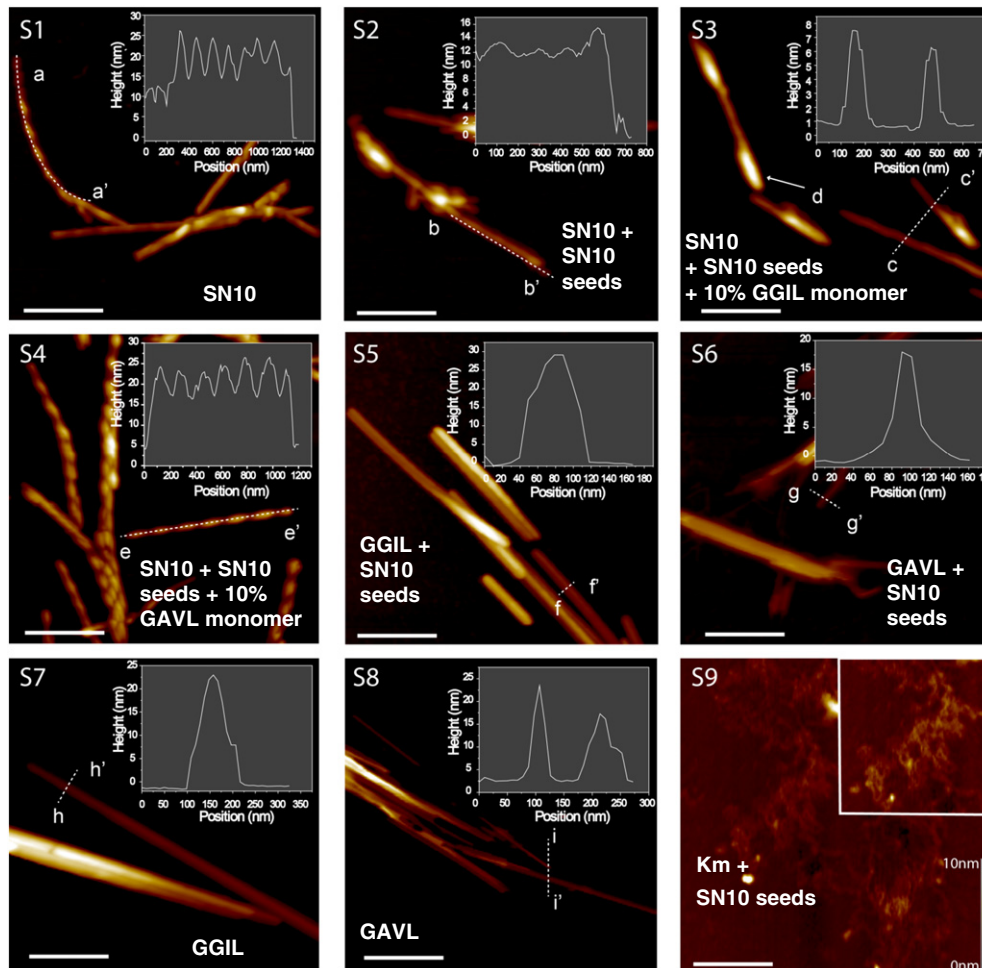


Fig. 8. Morphology of fibrils examined by atomic force microscopy: Upper panel: S1: Fibrils of SN10; S2: Fibrils of SN10 formed in the presence of 5% fibril seeds; S3: Fibrils of SN10 formed in the presence of 5% fibril seeds and 10% GGIL. Middle panel: S4: Fibrils of SN10 formed in the presence of 5% fibril seeds and 10% GAVL; S5: Fibrils of GGIL formed in the presence of 5% SN10 fibril seeds; S6: Fibrils of GAVL formed in the presence of 5% SN10 fibril seeds. Bottom panel: S7: Fibrils of GGIL; S8: Fibrils of GAVL; S9: Fibrils of analog Km formed in the presence of 5% SN10 fibril seeds. The scale bar represents 2 μ m. The insets are the line profiles along the dash lines. For S3, the arrow d highlights the special structure, which is similar to that seen in the TEM image. For S9, the inset is a zoomed in image.

observed for all SN10 fibrils, even those formed in the presence of peptide analogs and peptide mutants. This indicated that the SN10 peptide dictates the overall morphology of the fibrils, even though the mutants or the analogs have been incorporated into the fibrils and give rise to differences in the secondary structure of the fibrils. AFM images indicate a fibril height of 10–30 nm. This could indicate that several protofibrils wind around each other to form the final fibrils. The structure indicated by the arrow in Fig. 8 subpanel 3 could also reflect fibril fragments stacking on top of each other. Fibrils of analog Km made from elongation of preformed SN10 fibril seeds have a

morphology very unlike the morphology of the SN10 fibrils, displaying shorter and thinner fibrils that appear to bundle together or branch. We conclude that although analog Km is able to elongate fibril seeds and hence form the hydrogen bonding pattern needed for fibril formation, this bonding pattern is different from that formed by the parent peptide during fibrillation, and this in turn leads to different fibril morphologies.

The long, un-branched ribbon-like morphology is also observed for fibrils formed from the peptide mutants GGIL and GAVL. However, fibrils formed from both these mutants lack the twisting of the fibrils. A possible reason for this is that the stacking pattern of fibrils into ribbons is disturbed by the removal of the methyl groups in the mutants, reducing the strength of hydrophobic interactions at that position in the peptide and therefore altering the structures formed. In the mutant GGIL it could also be due to the introduction of more rotational freedom in the backbone by the A \rightarrow G mutation.

4. Discussion

We have investigated the consequences of interfering with a single peptide bond in the structure of an amyloidogenic peptide. The perturbations can be ranked as GGIL \approx GAVL < analog Km < analogs He, Nm and Rp, in terms of their ability to reduce fibrillation in the modified peptide. This is consistent with the degree of chemical modification of the peptide backbone, where the smallest changes are introduced in analog Km and the greatest degree of perturbation can be

Table 3

Summary of the morphology of fibrils as obtained from TEM and AFM images.

	Monomer	Wt seeds	Structure ^a	Periodicity (nm)	Height (nm)
1	SN10	×	F, uB, TR	~14	~26/~12
2	SN10	✓	F, uB, TR	~150	~13/~9
3	9SN10:1GGIL	✓	F, uB, TR	NA	6–10
4	9SN10:1GAVL	✓	F, uB, TR	14–20	~25/~17
5	GGIL	✓	F, uB, S	NA	20–30
6	GAVL	✓	F, uB, S	NA	16–20
7	GGIL	×	F, uB, S	NA	22–30
8	GAVL	×	F, uB, S	NA	17–24
9	Analog Km	✓	–	NA	NA

Notes:

^a F: fibrils; uB: un-branched; TR: Twisted ribbon like; S: Sheet like.

found in analog Rp followed by analogs He and Nm. It could be conceived that the exchange of a NH with a methylene group in the backbone as for Km would structurally alter the peptide due to the loss of orbital overlap of the nitrogen lone pair and the π^* orbital of the connecting carbonyl and hence loss of the double bond character for this particular linkage. Yet, this NH to CH₂ substitution should nevertheless impart only a minimal sterical increase for this linkage compared to the other modifications, since the carbon center, although being completely sp³ hybridized, only possesses one additional hydrogen atom compared to that of the wild-type peptide. Due to the absence of the double bond character in Km at one of the peptide linkages, this analog would display a higher degree of rotational freedom around this particular bond and hence greater flexibility. This could explain why Km cannot fibrillate on its own, but nevertheless easily adapts a conformation similar to that of SN10 in the fibrillation process with seeding of this wild-type peptide. On the other hand, the peptide analogs He and Nm show greater structural difference with either lack of the carbonyl group or increase sterical demand through the introduction of a methyl group on the nitrogen of the linkage, respectively. Combined with the fact that these peptide derivatives are shorter than SN10, this rationalizes their inability to fibrillate even with fibril seeding. Even though none of the peptides or mutants tested had the ability to inhibit fibrillation of the parent peptide, the analogs that could elongate seeds of the parent peptide were able to alter the fibril structure of the parent peptide upon incorporation of the analog/mutant into the SN10 fibrils formed. A similar polymorphism of the fibrils can also be seen for the fibrillating peptide hormone glucagon which has been found to adapt different fibril structures depending on fibrillation conditions [40–43] and mutations [44]. Glucagon is able to fibrillate over a wide range of conditions, because the backbone is intrinsically disposed toward fibrillation, reducing the fibrillation challenge to one of finding the structure that fits the current fibrillation conditions. The same effects can be observed for a 20 residue fragment of hIAPP when the amino acid is reversed and scrambled. This still leads to formation of amyloid like fibrils but the structure and properties of the aggregates differ from those of the original peptide [45]. In the present study all the analogs except analog Km lead to the fibrils being too destabilized by the modification to allow elongation to occur. This indicates that we have “overstepped the mark”, so that the analogs are not just unable to elongate existing fibrils, but they cannot even bind strongly enough to the fibrils to prevent binding of the non-analog peptides.

In contrast, the two side-chain mutants of SN10 (GGIL and GAVL), which were designed to mimic the increased backbone flexibility in the three analogs He, Nm and Rp and probe the effect of removing a methyl group, were able to form fibrils. Further, the kinetics of fibrillation of GGIL was not affected by the presence of fibril seeds of the wt peptide SN10. This could be ascribed to a higher aggregation propensity of this peptide as compared to the wt peptide. Gratifyingly, the aggregation propensity prediction software Zyggregator [8,46] found GGIL to have an aggregation propensity which exceeded the aggregation propensities of the two other peptides with approximately 0.2 units for the majority of the amino acid residues of the sequence (Fig. 9). Although GAVL has a slightly higher aggregation propensity than SN10 for all residues but the initial 3 (SNN), these two peptides are in general very similar with regards to aggregation propensity. Solid state NMR, FTIR and far-UV CD data also concur that GAVL (a side chain modification) is closer in structure to SN10 than GGIL (an increase in backbone flexibility as well as side chain modification). Thus, the two mutants promote the amyloidogenicity in a ranking order reflecting conformational perturbation of the backbone, while chemical backbone modifications either reduce it or completely eliminate it.

The difference in critical aggregation concentration between SN10 and NF6 is more than 100-fold, corresponding to a difference in fibrillation energy of 3.0 kcal/mol. This value is in the range of several hydrogen bonds [47], in good agreement with the fact that the shorter

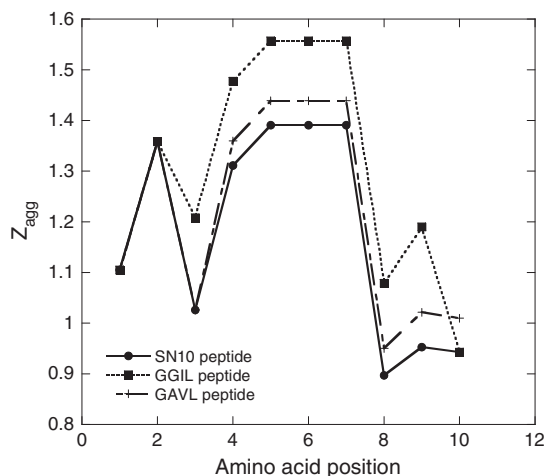


Fig. 9. Prediction of aggregation propensities of SN10, GGIL and GAVL made with the Zyggregator software [8,46]. The aggregation propensity of GGIL is higher than the other peptides examined in the present study.

NF6 peptide can be expected to have fewer hydrogen bonds between the individual peptide stands in the amyloid β -sheet. However the 0.5 kcal/mol difference in fibril stability between SN10 and analog Km is significantly less than the energy of a hydrogen bond. This is less than expected, given that one backbone amide group is removed from analog Km as compared to SN10. It is possible that rearrangements in the structure of the analog Km-containing fibrils (which are seen both at the level of secondary structure, apparent loss of the ~ 4.6 Å reflection in diffraction patterns as well as in terms of ultrastructure) compensate for the loss of this hydrogen bond by additional van der Waals interactions. The asymmetric nature of a fibril with anti-parallel hydrogen bonding between the β -strands, means that the same side chain experiences four different environments in different peptide molecules (Fig. 10 and Ref. [28]), and thus a single amino acid substitution can have different effects in different environments, and also lead to different structural rearrangements in different locations. All this will have unpredictable stability consequences. However, some conclusions can be made. The difference in c_c between SN10 and the two mutants translates to only 0.2–0.3 kcal/mol, and may be attributed to loss of hydrophobic interactions by the shortening of the Ala and the Ile respectively by a methyl group in the two mutants. These losses are very modest compared to the effect of methyl group removal from the core of globular proteins [48], indicating that the fibril structure does not pack these methyl groups very efficiently, so that few stabilizing interactions are lost upon their removal. This is confirmed by the structure of the peptide in the fibrils, cf. Fig. 10, where each side chain is found both point into the zipper and out toward the solvent, making fewer interactions. Furthermore, a loose packing of the side chains around both Ala and Gly is observed in one of the geometries. Altogether these factors indicate that the removal of a hydrophobic interaction will not have as severe an effect as that seen in e.g. globular proteins.

Peptoids have also been suggested as inhibitors of protein–protein interactions including fibrillation [49]. Furthermore they have the advantage of being protease resistant [31]. However, the results obtained for analog Rp, the retropeptoid version of SN10, are in accordance with the previous observation that the SN10 retropeptoid was not capable of forming amyloid structures on its own [32]. The limited inhibitory effect of the retropeptoid in a 1:1 mixture with SN10 could explain why no inhibitory effect is seen for analog Rp in this study where the ratio of SN10 to retropeptoid is 10:1. Previously developed β -breaker peptide analogs of SN10 comprise double backbone N-methylation which blocks the hydrogen-bonding pattern between

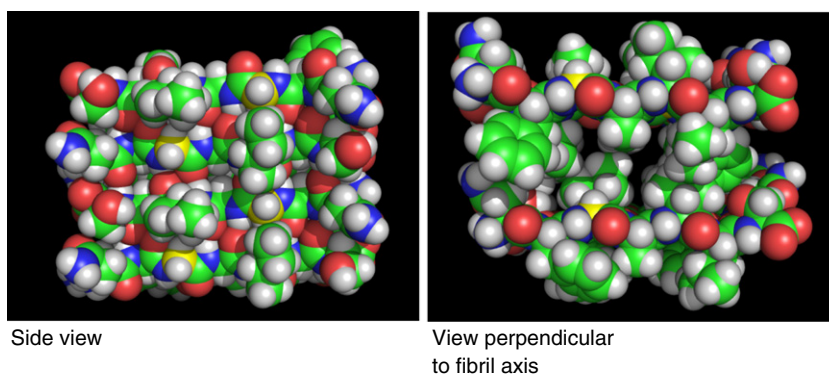


Fig. 10. Space fill model of the structure of the NFGAILS fragment of SN10 fibrils [28] showing the side-chain stacking and interactions between individual strands of the hetero zipper. The fibril is seen in a side view and a view perpendicular to the fibril axis. In the side view the fibril axis progresses from the top to the bottom. The color coding is C-atoms: green, N-atoms: blue, O-atoms: red, H-atoms: gray. The C α of Gly is shown in yellow. A loose packing around Gly is seen in every second strand of the fibril.

individual peptides by removal of the hydrogen donor site found in the backbone amid-groups [18,19]. Even though no inhibitory effect is seen for the N-methylated variant of NF6 on the fibrillation of the parent peptide, this variant is also not capable of elongating fibril seeds. This indicates that the introduction of a backbone N-methylation affects the ability of the NF6 peptide to form the hydrogen bonds needed to form amyloid fibrils. Furthermore, the inhibition of fibrillation of the parent peptide by addition of N-methylated analog required a 1:1 ratio of analog and parent peptide, which is a ~5 times higher fraction of the analog than what was used in the present study. The N-methylated analogs used in earlier studies were not able to inhibit the fibrillation of full length hIAPP [19]. These results are in good agreement with the results presented here.

The results presented here indicate that the peptide backbone structure is very important for the formation of amyloid fibrils. This can be ascribed to the hydrogen bonding pattern of individual peptides or β -strands in the amyloid fibrils being of utmost importance for stabilizing the amyloid structure. This is consistent with the high degree of persistence observed for stacking of individual β -strands in the fibril structure [12]. We have thus shown that amyloid fibrils do not form spontaneously when backbone integrity is compromised.

Acknowledgements

This work is supported by the Danish National Research Foundation (inSPIN). The authors would like to thank Dr Louise Serpell for helpful discussions and Dr. Michele Vendruscolo for use of the Zyggregator programme. We acknowledge EMBL-Hamburg for its provision of synchrotron facilities for X-ray diffraction studies and we thank Dr. Victor Lamzin and Johanna Kallio for their assistance in using the X13 beamline.

References

- [1] J.W. Kelly, The alternative conformations of amyloidogenic proteins and their multi-step assembly pathways, *Curr. Opin. Struct. Biol.* 8 (1998) 101–106.
- [2] J.C. Rochet, P.T. Lansbury Jr., Amyloid fibrillogenesis: themes and variations, *Curr. Opin. Struct. Biol.* 10 (2000) 60–68.
- [3] A. Clark, G.J. Cooper, C.E. Lewis, J.F. Morris, A.C. Willis, K.B. Reid, R.C. Turner, Islet amyloid formed from diabetes-associated peptide may be pathogenic in type-2 diabetes, *Lancet* 2 (1987) 231–234.
- [4] P. Westermark, M.D. Benson, J.N. Buxbaum, A.S. Cohen, B. Frangione, S. Ikeda, C.L. Masters, G. Merlini, M.J. Saraiva, J.D. Sipe, A primer of amyloid nomenclature, *Amyloid* 14 (2007) 179–183.
- [5] C.M. Dobson, Protein misfolding, evolution and disease, *Trends Biochem. Sci.* 24 (1999) 329–332.
- [6] K.F. DuBay, A.P. Pawar, F. Chiti, J. Zurdo, C.M. Dobson, M. Vendruscolo, Prediction of the absolute aggregation rates of amyloidogenic polypeptide chains, *J. Mol. Biol.* 341 (2004) 1317–1326.
- [7] F. Chiti, M. Stefani, N. Taddei, G. Ramponi, C.M. Dobson, Rationalization of the effects of mutations on peptide and protein aggregation rates, *Nature* 424 (2003) 805–808.
- [8] G.G. Tartaglia, A.P. Pawar, S. Campioni, C.M. Dobson, F. Chiti, M. Vendruscolo, Prediction of aggregation-prone regions in structured proteins, *J. Mol. Biol.* 380 (2008) 425–436.
- [9] A.M. Fernandez-Escamilla, F. Rousseau, J. Schymkowitz, L. Serrano, Prediction of sequence-dependent and mutational effects on the aggregation of peptides and proteins, *Nat. Biotechnol.* 22 (2004) 1302–1306.
- [10] M.R. Sawaya, S. Sambashivan, R. Nelson, M.I. Ivanova, S.A. Sievers, M.I. Apostol, M.J. Thompson, M. Balbirnie, J.J.W. Wiltzius, H.T. McFarlane, A.Ø. Madsen, R. Riek, D. Eisenberg, Atomic structures of amyloid cross- β spines reveal varied steric zippers, *Nature* 447 (2007) 453–457.
- [11] R. Nelson, M.R. Sawaya, M. Balbirnie, A.Ø. Madsen, C. Riek, R. Grothe, D. Eisenberg, Structure of the cross-beta spine of amyloid-like fibrils, *Nature* 435 (2005) 773–778.
- [12] T.P.J. Knowles, J.F. Smith, A. Craig, C.M. Dobson, M.E. Welland, Spatial persistence of angular correlations in amyloid fibrils, *Phys. Rev. Lett.* 96 (2006) 238301.
- [13] C. Soto, E.M. Sigurdsson, L. Morelli, R.A. Kumar, E.M. Castano, B. Frangione, Beta-sheet breaker peptides inhibit fibrillogenesis in a rat brain model of amyloidosis: implications for Alzheimer's therapy, *Nat. Med.* 4 (1998) 822–826.
- [14] G.M. Musso, C.C. Arico-Muendel, H.W. Benjamin, A.M. Hundal, J.-J. Lee, J. Chin, M. Kelley, J. Wakefield, N.J. Hayward, S.M. Molineau, Modified-peptide inhibitors of amyloid β -peptide polymerization, *Biochemistry* 38 (1999) 6791–6800.
- [15] S. Gilead, E. Gazit, Inhibition of amyloid fibril formation by peptide analogs modified with α -aminoisobutyric acid, *Angew. Chem. Int. Ed.* 116 (2004) 4133–4136.
- [16] L.O. Tjernberg, J. Naslund, F. Lindqvist, J. Johansson, A.R. Karlstrom, J. Thyberg, L. Terenius, C. Nordstedt, Arrest of beta-amyloid fibril formation by a pentapeptide ligand, *J. Biol. Chem.* 271 (1996) 8545–8548.
- [17] L.M. Yan, M. Tarek-Nossol, A. Velkova, A. Kazantzis, A. Kapurniotu, Design of a mimic of nonamyloidogenic and bioactive human islet amyloid polypeptide (IAPP) as nanomolar affinity inhibitor of IAPP cytotoxic fibrillogenesis, *Proc. Natl. Acad. Sci. U. S. A.* 103 (2006) 2046–2051.
- [18] A. Kapurniotu, A. Schmauder, K. Tenidis, Structure-based design and study of non-amyloidogenic, double N-methylated IAPP amyloid core sequences as inhibitors of IAPP amyloid formation and cytotoxicity, *J. Mol. Biol.* 315 (2002) 339–350.
- [19] M. Tarek-Nossol, L.M. Yan, A. Schmauder, K. Tenidis, G. Westermark, A. Kapurniotu, Inhibition of hIAPP amyloid-fibril formation and apoptotic cell death by a designed hIAPP amyloid-core-containing hexapeptide, *Chem. Biol.* 12 (2005) 797–809.
- [20] N. Kokkoni, K. Stott, H. Amijee, J.M. Mason, A.J. Doig, N-Methylated peptide inhibitors of beta-amyloid aggregation and toxicity. Optimization of the inhibitor structure, *Biochemistry* 45 (2006) 9906–9918.
- [21] D.T. Rijkers, J.W. Hoppener, G. Posthuma, C.J. Lips, R.M. Liskamp, Inhibition of amyloid fibril formation of human amylin by N-alkylated amino acid and alpha-hydroxy acid residue containing peptides, *Chemistry* 8 (2002) 4285–4291.
- [22] R.C. Elgersma, T. Meijneke, G. Posthuma, D.T. Rijkers, R.M. Liskamp, Self-assembly of amylin(20–29) amide-bond derivatives into helical ribbons and peptide nanotubes rather than fibrils, *Chemistry* 12 (2006) 3714–3725.
- [23] D.J. Gordon, K.L. Sciarretta, S.C. Meredith, Inhibition of beta-amyloid(40) fibrillogenesis and disassembly of beta-amyloid(40) fibrils by short beta-amyloid congeners containing N-methyl amino acids at alternate residues, *Biochemistry* 40 (2001) 8237–8245.
- [24] K. Tenidis, M. Waldner, J. Bernhagen, W. Fischle, M. Bergmann, M. Weber, M.L. Merkle, W. Voelter, H. Brunner, A. Kapurniotu, Identification of a penta- and hexapeptide of islet amyloid polypeptide (IAPP) with amyloidogenic and cytotoxic properties, *J. Mol. Biol.* 295 (2000) 1055–1071.
- [25] P. Westermark, U. Engstrom, K.H. Johnson, G.T. Westermark, C. Betsholtz, Islet amyloid polypeptide: pinpointing amino acid residues linked to amyloid fibril formation, *Proc. Natl. Acad. Sci. U. S. A.* 87 (1990) 5036–5040.
- [26] E.L. Opie, The relation of diabetes mellitus to lesions of the pancreas. Hyaline degeneration of the islands of Langerhans, *J. Exp. Med.* 5 (1901) 527–540.

- [27] G.J. Cooper, A.C. Willis, A. Clark, R.C. Turner, R.B. Sim, K.B. Reid, Purification and characterization of a peptide from amyloid-rich pancreases of type 2 diabetic patients, *Proc. Natl. Acad. Sci. U. S. A.* 84 (1987) 8628–8632.
- [28] J.T. Nielsen, M. Bjerring, M. Jeppesen, R.O. Pedersen, J.M. Pedersen, K.L. Hein, T. Vosegaard, T.S. Skrydstrup, D.E. Otzen, N.C. Nielsen, Unique identification of supramolecular structures in amyloid fibrils by solid-state NMR, *Angew. Chem. Int. Ed.* 48 (2009) 2118–2121.
- [29] J. Madine, E. Jack, P.G. Stockley, S.E. Radford, J.C. Serpell, D.A. Middleton, Structural insights into the polymorphism of amyloid-like fibrils formed by region 20–29 of amylin revealed by solid-state NMR and X-ray fiber diffraction, *J. Am. Chem. Soc.* 130 (2008) 14990–15001.
- [30] R.J. Simon, R.S. Kania, R.N. Zuckermann, V.D. Huebner, D.A. Jewell, S. Banville, S. Ng, L. Wang, S. Rosenberg, C.K. Marlowe, D.C. Spellmeyer, R. Tans, A.D. Frankel, D.V. Santi, F.E. Cohen, P.A. Bartlett, Peptoids: a modular approach to drug discovery, *Proc. Natl. Acad. Sci. U. S. A.* 89 (1992) 9367–9371.
- [31] S.M. Miller, R.J. Simon, S. Ng, R.N. Zuckermann, J.M. Kerr, W.H. Moos, Comparison of the proteolytic susceptibilities of homologous L-amino acid, D-amino acid, and N-substituted glycine peptide and peptoid oligomers, *Drug Dev. Res.* 35 (1995) 20–32.
- [32] R.C. Elgersma, G.E. Mulder, J.A. Kruijtzter, G. Posthuma, D.T. Rijkers, R.M. Liskamp, Transformation of the amyloidogenic peptide amylin(20–29) into its corresponding peptoid and retropeptoid: access to both an amyloid inhibitor and template for self-assembled supramolecular tapes, *Bioorg. Med. Chem. Lett.* 17 (2007) 1837–1842.
- [33] D. Mittag, D.E. Otzen, N.C. Nielsen, T.S. Skrydstrup, Synthesis of a ketomethylene isostere of the fibrillating peptide SNNFGAILSS, *J. Org. Chem.* 74 (2009) 7955–7957.
- [34] W.C. Chen, P.D. White, *Fmoc Solid Phase Peptide Synthesis*, Oxford University Press, Oxford, 2000.
- [35] S. Makin, P. Sikorski, L. Serpell, CLEARER: a new tool for the analysis of X-ray fibre diffraction patterns and diffraction simulation from atomic structural models, *J. Appl. Crystallogr.* 40 (2007) 966–972.
- [36] A.M. Morris, M.A. Watzky, R.G. Finke, Protein aggregation kinetics, mechanism, and curve-fitting: a review of the literature, *Biochim. Biophys. Acta* 1794 (2009) 375–397.
- [37] J.T. Jarrett, P.T. Lansbury Jr., Seeding “one-dimensional crystallization” of amyloid: a pathogenic mechanism in Alzheimer’s disease and scrapie? *Cell* 73 (1993) 1055–1058.
- [38] A. Peim, P. Hortschansky, T. Christopeit, V. Schroeckh, W. Richter, M. Fandrich, Mutagenic exploration of the cross-seeding and fibrillation propensity of Alzheimer’s beta-amyloid peptide variants, *Protein Sci.* 15 (2006) 1801–1805.
- [39] M. Sunde, L. Serpell, M. Bartlam, P. Fraser, M. Pepys, C. Blake, Common core structure of amyloid fibrils by synchrotron X-ray diffraction, *J. Mol. Biol.* 273 (1997) 729–739.
- [40] J.S. Pedersen, C.B. Andersen, D.E. Otzen, Institutional nonconformism: the many levels of glucagon polymorphism, *FEBS J.* 277 (2010) 4591–4601.
- [41] C.B. Andersen, M.R. Hicks, B. Vandahl, H. Rahbek-Nielsen, H. Thøgersen, I.B. Thøgersen, J.J. Enghild, L.C. Serpell, C. Rischel, D.E. Otzen, Glucagon fibril polymorphism reflects differences in protofilament backbone structure, *J. Mol. Biol.* 397 (2010) 932–946.
- [42] J.S. Pedersen, D. Dikov, J.L. Flink, H.A. Hjuler, G. Christiansen, D.E. Otzen, The changing face of glucagon fibrillation: structural polymorphism and conformational imprinting, *J. Mol. Biol.* 355 (2006) 501–523.
- [43] J.S. Pedersen, D.E. Otzen, Amyloid – a state in many guises: survival of the fittest fibril fold, *Protein Sci.* 17 (2008) 1–9.
- [44] J.S. Pedersen, D. Dikov, D.E. Otzen, N- and C-terminal hydrophobic patches are involved in fibrillation of glucagon, *Biochemistry* 45 (2006) 14503–14512.
- [45] R. Sabate, A. Espargaro, N.S. de Groot, J.J. Valle-Delgado, X. Fernandez-Busquets, S. Ventura, The role of protein sequence and amino acid composition in amyloid formation: scrambling and backward reading of IAPP amyloid fibrils, *J. Mol. Biol.* 404 (2010) 337–352.
- [46] G.G. Tartaglia, M. Vendruscolo, The Zyggregator method for predicting protein aggregation propensities, *Chem. Soc. Rev.* 37 (2008) 1395–1401.
- [47] A.R. Fersht, J.P. Shi, J. Knill-Jones, D.M. Lowe, A.J. Wilkinson, D.M. Blow, P. Brick, P. Carter, M.M.Y. Waye, G. Winter, Hydrogen bonding and biological specificity analysed by protein engineering, *Nature* 314 (1985) 235–238.
- [48] A.R. Fersht, S.E. Jackson, L. Serrano, Protein stability: experimental data from protein engineering, *Phil. Trans. R. Soc. Lond.* 345 (1993) 141–151.
- [49] R. Ruijtenbeek, J.A. Kruijtzter, W. van de Wiel, M.J. Fischer, M. Fluck, F.A. Redegeld, R.M. Liskamp, F.P. Nijkamp, Peptoid – peptide hybrids that bind Syk SH2 domains involved in signal transduction, *ChemBioChem* 2 (2001) 171–179.
- [50] J. Kong, S. Yu, Fourier transform infrared spectroscopic analysis of protein secondary structures, *Acta Biochim. Biophys. Sin. (Shanghai)* 39 (2007) 549–559.
- [51] G. Zandomenighi, M.R. Krebs, M.G. McCammon, M. Fandrich, FTIR reveals structural differences between native beta-sheet proteins and amyloid fibrils, *Protein Sci.* 13 (2004) 3314–3321.